

Classification of rain events using directional radio data of commercial microwave links

1st Fabian Kovac

Center for Artificial Intelligence
St. Pölten University of Applied Sciences, Austria
fabian.kovac@fhstp.ac.at

2nd Oliver Eigner

Center for Artificial Intelligence
St. Pölten University of Applied Sciences, Austria
oliver.eigner@fhstp.ac.at

3rd Alexander Adrowitzer

Center for Artificial Intelligence
St. Pölten University of Applied Sciences, Austria
alexander.adrowitzer@fhstp.ac.at

4th Hubert Schölnast

Center for Artificial Intelligence
St. Pölten University of Applied Sciences, Austria
hubert.schoelnast@fhstp.ac.at

5th Alexander Buchelt

Center for Artificial Intelligence
St. Pölten University of Applied Sciences, Austria
alexander.buchelt@fhstp.ac.at

Abstract—Due to climate change, more and more extreme weather events are occurring. An accurate short-term forecast in terms of time and location represents a significant advantage for taking appropriate measures to prevent damage and to react and plan more efficiently. This requires a network of ground stations or remote sensing systems such as weather radar or satellites as dense as possible. In large parts of Austria, however, rough terrain limits the number of measuring stations and radar data are also only available to an insufficient extent in certain areas due to the topography. We aim to overcome these challenges by using physical data of directional radio links scattered across Austria to obtain information about the current precipitation situation. In this work, we introduce an approach for classifying rain events using a variety of different machine learning methods. The results can be used to improve numerical weather prediction models.

Keywords—machine learning, classification, commercial microwave links

I. INTRODUCTION

Short-term forecasts of extreme weather events are an increasingly important basis for decision-making due to climate change, both for economic measures and for measures to ensure the safety of the population. Due to climate change, more and more extreme weather events are occurring. An accurate short-term forecast in terms of time and location represents a significant advantage for taking appropriate measures to prevent damage and to react and plan more efficiently. The quality of these forecasts can profit from the wide availability of measurement data provided by commercial microwave links (CML). Short-term forecasts require a reasonably dense network of ground stations or remote sensing systems such as weather radar or satellites to provide current weather data.

In many parts of several countries, however, the number of ground stations is limited due to rough terrain, while radar data may be lacking for certain regions due to topographical reasons [1].

To overcome these limitations, commercial microwave links provided by mobile network operators as a complement to satellites and weather radars, as well as ground stations currently deployed over different parts of the world. A major advantage of using existing infrastructure of mobile operators, like CMLs, lies not only in the cost-effectiveness but also in their data recording capabilities. Said data can be used in numerical models to complete rain monitoring provided by rain gauges and weather stations. Thus, retrieval of precipitation data from CML data and subsequent mapping is a form of opportunistic weather forecasting that has become increasingly important in the research area of meteorology and geodynamics in recent years [2] [3].

A. Related work

The difficulty of precipitation estimation from CML data is to distinguish between fluctuations of raw attenuation data during dry and wet periods. In the available literature, this issue has already been addressed using various approaches. Microwave signals with frequencies from about 1 to 100 GHz (about 0.3 cm to 30 cm wavelength) are attenuated as they travel through the atmosphere. This attenuation depends primarily on the rain density and humidity along the microwave links path and was observed even before radio technology even worked in this frequency range [4]. Since then, studies have been conducted repeatedly to estimate precipitation between the CML transmitter and receiver (see, e.g., [5] [6] [7]). Other studies addressed the creation of gridded precipitation fields [8], relative humidity [9]), and

even rain drop size distribution [10]. Precipitation data from CMLs have been obtained, for example, by spatial correlation of precipitation [11] or analysis of individual time series [2] [12]. A combination with other observations is also possible [13] [14]. Furthermore, CMLs have been applied for hydrological purposes such as urban drainage or runoff modeling [15] [16]. Larger datasets have been used, for example, to produce two years of precipitation data for the Netherlands [11] or an estimate over all of Germany [10]. Recently, there have also been early attempts to use artificial intelligence for forecasting weather and/or precipitation events. Naveen and Mohan [17] provide a very good overview of persistent, synoptic, statistical, and computer-generated forecasting. Current studies dealing with atmospheric weather forecasting using various machine learning techniques are compared. Booz et al. [18] explored a deep learning approach for a weather forecasting system. The authors defined a deep learning model to build a neural network for forecasting. Another approach [19] uses a neural network for weather analysis and rain rate prediction with high accuracy. The authors of [20] use a classical Linear Discriminant Analysis to classify transmission data between two microwave links in a 3-day period into four classes of precipitation. A similar classification using cell phones in a 4G/LTE network is described by Beritelli et al. [21] using a probabilistic neural network. The database was collected only between a cell phone and a base station in a period of 112 hours to establish a first proof of concept. Ravuri et al [22] show another method by exploring a deep generative model for likelihood-based prediction of precipitation from radar using statistical, economic, and cognitive measures. Their model produces realistic and spatiotemporally consistent forecasts over regions. The authors have shown that generative nowcasting can provide probabilistic forecasts that improve predictive value and support operational utility, at resolutions and lead times where alternative methods struggle. Despite all these research studies [23] [11] [24] [25] [26] indicating the potential of CMLs for rainfall determination, challenges still remain. These mainly concern the handling of typical sources of error, e.g. the wetting of antennas during rain events or dense fog [27] leading to an additional attenuation and therefore to an overestimation of the precipitation amount, as well as decreasing signal levels during dry periods.

The outline of this paper is as follows. First, available commercial microwave link data are described including preparation steps taken and features used for classification. The main part of the paper deals with the experimental setup including the baseline and final model used for classifying rain events. Finally, the conclusion summarizes the results and future work highlights the recommendations and outlooks for further research.

II. DATA PREPARATION

A. Commercial Microwave Links

The study area considered is Austria ($\approx 83.900 \text{ km}^2$) and approximately one quarter of the country's area is located on lowlands and hilly areas. Only 32% of the area lie below an altitude of 500 hm and more than 70% of the national territory is mountainous [28].

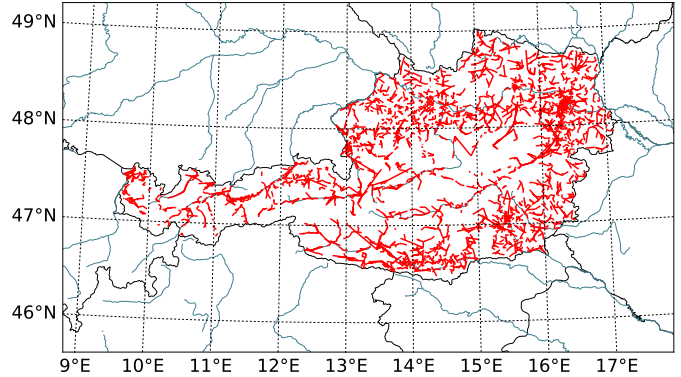


Fig. 1. Commercial Microwave Links scattered over Austria

TABLE I
CMLs BASED ON OPERATING FREQUENCY BAND INCLUDING AVERAGE PATH LENGTHS

Frequency [GHz]	# CML	Average Path Length [km]
13	141	14.7
18	239	9.1
23	444	6.9
26	231	5.9
28	14	2.3
38	56	1.6
80	3440	1.6

As seen in figure 1, the CMLs distributed over Austria have a high temporal and spatial data availability which, in conjunction with the country's topographical properties, make Austria a representative example using microwave links to estimate rain events. The data available were obtained by Hutchison Drei Austria GmbH and range from May 2021 to February 2022. Sent and received powers of microwave links as well as their operating frequency bands (listed in table I) are obtained over 3-minute intervals and aggregated to 15-minute intervals to extract minimum, maximum and mean power levels respectively. Lengths of the microwave links are calculated using their geographical locations afterwards using a WGS-84 rotational ellipsoid.

To verify the results of the CML models, actual rainfall data provided by the Austrian Central Institution for Meteorology and Geodynamics (ZAMG) are used. These are data on actual rainfall, precipitation type, wind strength and directions, observations from individual weather stations as

well as 2m temperature and 2m humidity (temperature and humidity measured two metres above the ground), which are available with a temporal resolution of 15 minutes for a 1 km grid over Austria and beyond the national borders.

B. Feature Engineering

To gain further insights about signal attenuations at given times, the extinction coefficient (also often referred to attenuation coefficient) [29] is calculated to describe the extinction of the signal caused by the attenuation and the length of the microwave links using the Beer-Lambert law [30], which describes the attenuation of the signal with respect to its initial intensity when passing through a medium containing an absorbing substance (air) and the layer thickness (length of the CML).

Given the sent power S_0 and received power S of the 15-minute interval, the attenuation D can be calculated with

$$D = S - S_0. \quad (1)$$

This attenuation is also the decadic logarithm of the ratio of two intensities

$$D = 10 \cdot \log_{10}\left(\frac{I}{I_0}\right), \quad (2)$$

where I_0 and I describe the intensity of the radiation (in W) of the sender and receiver respectively.

If there is a (reasonably) homogeneous medium between the emitter (transmitter) and the detector (receiver), which is the cause of the extinction, the intensity I_0 decays exponentially after passing through the absorbing medium of thickness l according to Beer-Lambert's law:

$$I = I_0 \cdot e^{-\alpha \cdot l} \quad (3)$$

Solving Beer-Lambert's law for α , which defines the material property of this absorption as the extinction coefficient, we obtain:

$$\alpha = -\frac{\ln\left(\frac{I}{I_0}\right)}{l} \quad (4)$$

The numerator of the fraction contains the attenuation as seen in equation (2), only with the logarithm of a different base:

$$\ln\left(\frac{I}{I_0}\right) = \ln(10) \cdot \log_{10}\left(\frac{I}{I_0}\right) = \ln(10) \cdot \frac{D}{10} \quad (5)$$

If we now put this back into equation (4) resolved according to α , the coefficient can be calculated from the attenuation and the length of CMLs:

$$\alpha = -\frac{\ln(10)}{10} \cdot \frac{D}{l} = -0.23 \cdot \frac{D}{l} \quad (6)$$

This makes it possible to combine three of the most important characteristics of available CML data (sending and receiving signal powers and the length of the link) into a single coefficient, which in conjunction with the standard deviation of attenuation in the 15-minute interval as well as frequency proved to be very influential for the machine learning process.

While a differentiation based on the state a CML operates is not optimal considering Austria's topography, we defined a 10 km^2 grid and combined these grid points into clusters (see figure 2) depending on the topographical properties. This data is then used as categorical feature to categorize links based on Austria's topography.

The final feature set with corresponding units is listed in table II.

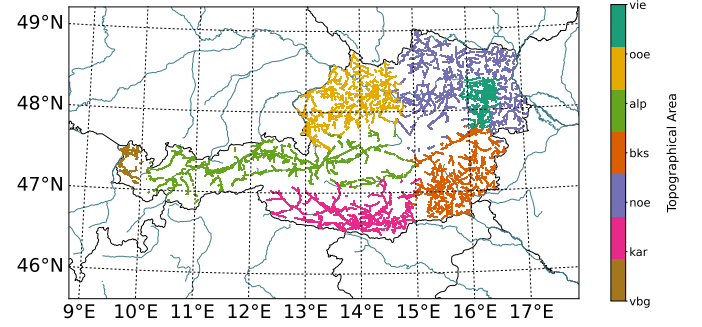


Fig. 2. Commercial Microwave Links based on topographical area

TABLE II
AVAILABLE FEATURES FOR CLASSIFICATION

Name	Unit	Description
DateTime	UTC	Datetime of the recording
RxLevel	dBm	Min/max received power levels
TxLevel	dBm	Min/max sent power levels
Attn	dB	Min/max attenuations
AttnDiff	dB	Min/max Attn deviation to dry periods
AttnStd	dB	Attn standard deviation
AttnMeanDry	dB	Mean attenuation during dry periods
AttnMeanStd	dB	Attn standard deviation during dry periods
ExtinctionCoeff	m^{-1}	Min/max extinction coefficient
RxBitrate	bit/s	Min/max received bitrate
TxBitrate	bit/s	Min/max sent bitrate
RxProfile	categorical	Min/max receiving profile used
TxProfile	categorical	Min/max sending profile used
PathLength	km	Length of Microwave Link
Frequency	GHz	Frequency used during transmission
Area	categorical	Area based on Austria's topography

III. EXPERIMENTAL SETUP

A. Environment

Our development environment consists of miniforge¹, an open source conda environment including *Python 3.9.6* and *scikit-learn 1.0*. Using this environment, we developed our models, which are able to predict rain events with precipitation greater than 0.01 mm/15 min using Commercial Microwave Link data.

¹<https://github.com/conda-forge/miniforge>

B. Setup

Preprocessed data as described in section II-B ranging from May 2021 to October 2021 are labeled based on the ground truth using radar data providing actual precipitation in mm/15 min. This data set includes CML observations during dry periods, extreme events such as thunderstorms and everything in between to ensure a wide variation of weather events.

Radar data is available in form of a grid of $701 \times 401 \text{ km}^2$ over Austria where each data point provides the actual rain rate at given location. While signal power observations of Commercial Microwave Links are only available at the sending and receiving end respectively, it is impossible to tell where a rain event is located on the links path. Therefore per *km* of CMLs *PathLength*, links are divided into uneven observation points as this always provides an observation point for the midpoint on the CML, where the actual rain rates based on the radar grid on the INCA forecasting model [31] are considered as ground truth. This *RRPath* with precipitation along microwave links is summed up where values $< 0.01 \text{ mm/15 min}$ are labeled as $[0 : \textit{Dry}]$ and remaining values are labeled $[1 : \textit{Rain}]$. As there are much more observed dry events than rain events, we draw random samples with equal distribution between the two classes.

Next labeled data is split into a train- (80%) and test-set (20%) using stratified sampling to get equal distributions between the labels itself as well as *Frequency* and *Area* CMLs operate in. The train-set is then fed through the training pipeline using 10-fold cross-validation and gridsearch to find the best parameter combinations. Data is normalized, *Area* as categorical feature is one-hot encoded and *DateTime* (month and hour) are cyclic feature encoded using (co-)sinusoidal waves during this process to model the month and hour of observations.

Results are evaluated using common machine learning metrics such as Accuracy, Precision, Recall and Cohen's Kappa. After finding the best model and parameter combination, Likelihood-ratio tests provides further insights about the best found model and quality of the results.

C. Baseline Model

While the machine learning pipeline stays exactly the same for our step-wise approach to update and harden the model, first only Commercial Microwave Links of our defined area *ooe* as seen in figure 2, including Upper Austria and northern parts of Salzburg, were considered as a subset to develop a baseline model. This subset consists of 815 CMLs spanning an area of $\approx 340 \text{ km}^2$ with homogeneous topographical properties. This baseline model serves as a fast sandbox for testing the feasibility with different data preparation steps and engineered features. In order to facilitate these tests and using the setup as described in section III-B, a Logistic Regression (LogR) fit with Stochastic Gradient Descent was chosen as it is one of the oldest classifiers working in a time effective manner. The best parameter combination was able to correctly classify rain events with an accuracy of over 97% (see table III for all metrics).

TABLE III
CLASSIFICATION METRICS, SCORES AND CONFUSION MATRIX FOR THE BASELINE MODEL

Metric	Score	Predicted	
		rain	dry
Accuracy	0.979		
F1	0.972		
Precision	0.989		
Recall	0.956		
Cohen's κ	0.956		
Support	$1.2e5$		
λ_{LR}	< 0.01		

Actual	Predicted	
	rain	dry
rain	TP 95.56%	FN 4.44%
dry	FP 0.63%	TN 99.37%

Figure 3 shows the output probabilities of the model for area *ooe* with INCA radar data as ground truth providing actual precipitation amounts for July 17th, 2021 at 4am during a severe thunderstorm weekend serving as a representative example of the model in action.

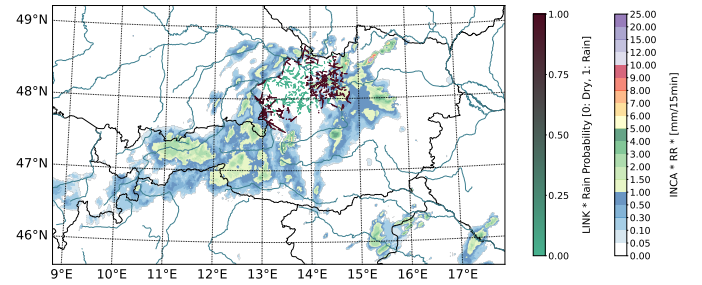


Fig. 3. Classified rain events considering a homogeneous subset by the baseline model with ground truth based on radar data during a thunderstorm weekend on July 17th, 2021 at 4am

D. Final Model

For the final model, all 4565 CMLs in Austria were considered spanning all topographical properties. We used and evaluated a variety of classification algorithms consisting of Logistic Regressions (LogR), Support Vector Machines (SVM) with linear and polynomial kernels, Decision Trees (DT) as well as Random Forests (RF). Classification metrics as well as the confusion matrix for the best model (RF) are shown in table IV. To ensure reproducibility, all models were trained using the same seed.

Tree-based algorithms like Decision Tree (DT) and the ensemble variant Random Forest (RF) outperform Logistic Regression (LogR) and Support Vector Machine (SVM) by a significant margin on all metrics. Logistic Regression on all available CMLs shows a noteworthy drop in performance when compared to the subset used during baseline modeling as described in section III-C. This is shown by a delta of at least ≈ 27 percentage points on all metrics which may be caused by considering all topographical properties instead of a homogeneous subset used in the baseline model.

We found the best model as a Random Forest (RF) which was able to correctly classify rain events with an accuracy of over 94%.

TABLE IV
CLASSIFICATION METRICS AND SCORES FOR THE FINAL MODEL AND
CONFUSION MATRIX FOR THE BEST MODEL (RF)

Metric	LogR	SVM	DT	RF
Accuracy	0.708	0.685	0.939	0.947
F1	0.533	0.439	0.913	0.931
Precision	0.672	0.672	0.983	0.947
Recall	0.442	0.326	0.853	0.915
Cohen's κ	0.733	0.756	0.866	0.888
Support	8.46 · 10 ⁵			
λ_{LR}	< 0.01			

		Predicted	
		rain	dry
Actual	rain	<i>TP</i> 89.93%	<i>FN</i> 10.07%
	dry	<i>FP</i> 3.84%	<i>TN</i> 96.16%

Figure 4 shows the output probabilities of the RF model for the whole country with INCA radar data as ground truth providing actual precipitation amounts. To compare the results with the baseline model, the same time frame with July 17th, 2021 at 4am during a severe thunderstorm weekend was used.

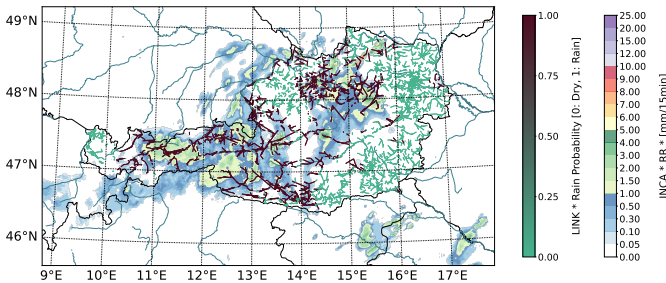


Fig. 4. Classified rain events considering all microwave links in Austria by the final model with ground truth based on radar data during a thunderstorm weekend on July 17th, 2021 at 4am

IV. CONCLUSION

Using data of Commercial Microwave Links, we show that classic machine learning approaches are able to correctly classify rain events with high accuracy and precision. With this approach, using Beer-Lambert's Law showed to be highly beneficial to extract relevant features for the classification task

to model material properties using the extinction coefficient. Independent of topographical properties and the severity of the corresponding weather phenomena, classified results were verified with ground truth radar data and could therefore be used to improve existing numerical weather models in a cost-effective manner by using data of already existing networks of mobile network providers.

Additionally, an added value for mobile network providers lies in the methods and insights gained in how the AI-supported combination of weather and directional radio data could be used to clearly assign outages and faults due to weather phenomena.

V. FUTURE WORK

While classification of wet/dry events is only the first step during this research project, predicting the actual rain rate [mm/15 min] as close as possible is pursued. Currently we indirectly measure how much liquid water is in the air in the form of droplets, but a determination of how much water actually falls to the ground for each 15 minute interval is pursued. If a certain attenuation is measured, the amount of rain falling on the ground depends on the square of droplet sizes. Droplet diameter varies between about 0.1 mm and 5 mm [32], a factor of 20. Therefore, for a given measured attenuation, the actual amount of rain can vary by a factor of 400. This inaccuracy is only mitigated by the fact that there is apparently a correlation between the amount of rain and the droplet size. However, this relationship is still insufficiently researched, where AI could be used to model this relationship.

Fog is also a problem still to be solved. When droplets are so small that they barely fall, they float in the air as mist. A small amount of liquid water that does not fall to the ground as rain causes a large extinction coefficient and therefore a large attenuation on CMLs, which at first glance cannot be distinguished from heavy rain using previous models. However, we have been able to determine that rain and fog cause different temporal patterns in space and can be distinguished in the future using AI.

At the moment, we are focusing on Austria, where topography varies from mountainous regions e.g. the Alps to low altitudes that can sometimes produce meteorological phenomena that are confined to relatively small geographic areas. Proposed methods can be extended to explore other regions with different meteorological characteristics.

All steps from gathering and preparation of the data at the mobile operator to the import into processing in numerical weather models are currently done on demand and manually. To eliminate sources of error and ensure smoother execution, these processes will be combined into an automated machine learning pipeline using CMLs acting as virtual weather balloons to support numerical weather models especially in regions, where the density of weather ground stations or radar data is sparse due to topographical properties. Learning could be incremental, updating the models as new CML observations arrive with the possibility of giving more priority to most recent data.

VI. ACKNOWLEDGEMENTS

This project is funded by the KIRAS program of the Austrian Research Promotion Agency (FFG). KIRAS funds projects in the field of smart natural disaster prediction, with machine learning being a subcategory in this context.

The project is carried out in cooperation with H3A and ZAMG as well as the hydrography unit of water management, resources and sustainability of the state Styria, Austria as requirements carrier.

REFERENCES

- [1] Q. Sun, C. Miao, Q. Duan, H. Ashouri, S. Sorooshian, and K.-L. Hsu, "A review of global precipitation data sets: Data sources, estimation, and intercomparisons," *Reviews of Geophysics*, vol. 56, no. 1, pp. 79–107, 2018. [Online]. Available: <https://agupubs.onlinelibrary.wiley.com/doi/abs/10.1002/2017RG000574>
- [2] C. Chwala and H. Kunstmann, "Commercial microwave link networks for rainfall observation: Assessment of the current status and future challenges," *WIREs Water*, vol. 6, no. 2, Mar. 2019.
- [3] R. Uijlenhoet, A. Overeem, and H. Leijnse, "Opportunistic remote sensing of rainfall using microwave links from cellular communication networks," *WIREs Water*, vol. 5, no. 4, p. e1289, 2018. [Online]. Available: <https://wires.onlinelibrary.wiley.com/doi/abs/10.1002/wat2.1289>
- [4] J. Stratton, "The effect of rain and fog on the propagation of very short radio waves," *Proceedings of the Institute of Radio Engineers*, vol. 18, no. 6, pp. 1064–1074, 1930.
- [5] A. Holt, G. Kuznetsov, and A. Rahimi, "Comparison of the use of dual-frequency and single-frequency attenuation for the measurement of path-averaged rainfall along a microwave link," *Microwaves, Antennas and Propagation, IEEE Proceedings*, vol. 150, pp. 315–20, 11 2003.
- [6] H. Leijnse, R. Uijlenhoet, and J. N. M. Stricker, "Rainfall measurement using radio links from cellular communication networks," *Water Resources Research*, vol. 43, no. 3, 2007.
- [7] A. Overeem, H. Leijnse, and R. Uijlenhoet, "Measuring urban rainfall using microwave links from commercial cellular communication networks," *Water Resources Research*, vol. 47, no. 12, 2011.
- [8] A. Zinevich, H. Messer, and P. Alpert, "Frontal Rainfall Observation by a Commercial Microwave Communication Network," *Journal of Applied Meteorology and Climatology*, vol. 48, no. 7, pp. 1317–1334, Jul. 2009.
- [9] N. David, O. Sendik, Y. Rubín, H. Messer, H. Gao, D. Rostkier-Edelstein, and P. Alpert, "Analyzing the ability to reconstruct the moisture field using commercial microwave network data," *Atmospheric research*, vol. 219, pp. 213–222, 2019.
- [10] M. Graf, C. Chwala, J. Polz, and H. Kunstmann, "Rainfall estimation from a german-wide commercial microwave link network: optimized processing and validation for 1 year of data," *Hydrology and Earth System Sciences*, vol. 24, no. 6, pp. 2931–2950, 2020. [Online]. Available: <https://hess.copernicus.org/articles/24/2931/2020/>
- [11] A. Overeem, H. Leijnse, and R. Uijlenhoet, "Retrieval algorithm for rainfall mapping from microwave links in a cellular communication network," *Atmospheric Measurement Techniques*, vol. 9, no. 5, pp. 2425–2444, Jun. 2016.
- [12] Z. Wang, M. Schleiss, J. Jaffrain, A. Berne, and J. Rieckermann, "Using markov switching models to infer dry and rainy periods from telecommunication microwave link signals," *Atmospheric Measurement Techniques*, vol. 5, no. 7, pp. 1847–1859, 2012. [Online]. Available: <https://amt.copernicus.org/articles/5/1847/2012/>
- [13] M. Fencel, M. Dohnal, J. Rieckermann, and V. Bareš, "Gauge-adjusted rainfall estimates from commercial microwave links," *Hydrology and Earth System Sciences*, vol. 21, no. 1, pp. 617–634, 2017. [Online]. Available: <https://hess.copernicus.org/articles/21/617/2017/>
- [14] Y. Liberman, R. Samuels, P. Alpert, and H. Messer, "New algorithm for integration between wireless microwave sensor network and radar for improved rainfall measurement and mapping," *Atmospheric Measurement Techniques*, vol. 7, no. 10, pp. 3549–3563, 2014. [Online]. Available: <https://amt.copernicus.org/articles/7/3549/2014/>
- [15] C. C. Brauer, A. Overeem, H. Leijnse, and R. Uijlenhoet, "The effect of differences between rainfall measurement techniques on groundwater and discharge simulations in a lowland catchment," *Hydrological Processes*, vol. 30, no. 21, pp. 3885–3900, 2016. [Online]. Available: <https://onlinelibrary.wiley.com/doi/abs/10.1002/hyp.10898>
- [16] D. Stransky, M. Fencel, and V. Bares, "Runoff prediction using rainfall data from microwave links: Tabor case study," *Water Science and Technology*, vol. 2017, no. 2, pp. 351–359, 04 2018. [Online]. Available: <https://doi.org/10.2166/wst.2018.149>
- [17] N. L. and M. H.S., "Atmospheric weather prediction using various machine learning techniques: A survey," in *2019 3rd International Conference on Computing Methodologies and Communication (ICCMC)*, 2019, pp. 422–428.
- [18] J. Booz, W. Yu, G. Xu, D. Griffith, and N. Golmie, "A deep learning-based weather forecast system for data volume and recency analysis," in *2019 International Conference on Computing, Networking and Communications (ICNC)*, 2019, pp. 697–701.
- [19] T. Anandharajan, G. A. Hariharan, K. Vignajeth, R. Jijendiran, and Kushmita, "Weather monitoring using artificial intelligence," in *2nd International Conference on Computational Intelligence and Networks (CINE)*, 2016, pp. 106–111.
- [20] D. Cherkassky, J. Ostrometzky, and H. Messer, "Precipitation classification using measurements from commercial microwave links," *IEEE Transactions on Geoscience and Remote Sensing*, vol. 52, no. 5, pp. 2350–2356, 2014.
- [21] F. Beritelli, G. Capizzi, G. Sciuto, F. Scaglione, D. Połap, and M. Woźniak, "A neural network pattern recognition approach to automatic rainfall classification by using signal strength in lte/4g networks," in *Rough Sets*. Springer International Publishing, 07 2017, pp. 505–512.
- [22] S. Ravuri, K. Lenc, M. Willson, D. Kangin, R. Lam, P. Mirowski, M. Fitzsimons, M. Athanassiadou, S. Kashem, S. Madge, R. Prudden, A. Mandhane, A. Clark, A. Brock, K. Simonyan, R. Hadsell, N. Robinson, E. Clancy, A. Arribas, and S. Mohamed, "Skilful precipitation nowcasting using deep generative models of radar," *Nature*, vol. 597, no. 7878, pp. 672–677, Sep. 2021. [Online]. Available: <https://www.nature.com/articles/s41586-021-03854-z>
- [23] H. Messer and O. Sendik, "A new approach to precipitation monitoring: A critical survey of existing technologies and challenges," *IEEE Signal Processing Magazine*, vol. 32, no. 3, pp. 110–122, 2015.
- [24] A. Overeem, H. Leijnse, T. van Leth, L. Bogerd, J. Priebe, D. Tricarico, A. M. Droste, and R. Uijlenhoet, "Tropical rainfall monitoring with commercial microwave links in Sri Lanka," *Environmental Research Letters*, 2021.
- [25] M. A. Samad, F. D. Diba, and D.-Y. Choi, "A Survey of Rain Attenuation Prediction Models for Terrestrial Links—Current Research Challenges and State-of-the-Art," *Sens*, vol. 21, no. 4, p. 1207, Feb. 2021.
- [26] K. Song, X. Liu, and T. Gao, "Real-time rainfall estimation using microwave links: A case study in east China during the plum rain season in 2020," *Sensors*, vol. 21, no. 3, p. 858, 2021.
- [27] M. Fencel, P. Valtr, M. Kvičera, and V. Bareš, "Quantifying wet antenna attenuation in 38-ghz commercial microwave links of cellular backhaul," *IEEE Geoscience and Remote Sensing Letters*, vol. 16, no. 4, pp. 514–518, 2019.
- [28] E. Gløersen, M. Price, H. Aalbu, E. Stucki, O. Roque, M. Schuler, and M. Perlik, *Mountain Areas in Europe: Analysis of Mountain Areas in EU Member States, Acceding and Other European Countries*. Nordregio, Nordic Centre for Spatial Development, Stockholm, Sweden: Nordregio, Jan. 2004.
- [29] T. S. Glickman and American Meteorological Society, *Glossary of Meteorology*, 2nd ed. Boston, Mass: American Meteorological Society, 2000.
- [30] V. Gold, Ed., *The IUPAC Compendium of Chemical Terminology: The Gold Book*, 4th ed. Research Triangle Park, NC: International Union of Pure and Applied Chemistry (IUPAC), 2019. [Online]. Available: <https://goldbook.iupac.org/>
- [31] E. Ghaemi, U. Foelsche, A. Kann, and J. Fuchsberger, "Evaluation of Integrated Nowcasting through Comprehensive Analysis (INCA) precipitation analysis using a dense rain-gauge network in southeastern Austria," *Hydrology and Earth System Sciences*, vol. 25, no. 8, pp. 4335–4356, Aug. 2021. [Online]. Available: <https://hess.copernicus.org/articles/25/4335/2021/>
- [32] P. T. Willis and P. Tattelman, "Drop-Size Distributions Associated with Intense Rainfall," *Journal of Applied Meteorology and Climatology*, vol. 28, no. 1, pp. 3–15, Jan. 1989. [Online]. Available: https://journals.ametsoc.org/view/journals/apme/28/1/1520-0450_1989_028_0003_dsdawi_2_0_co_2.xml